JOURNAL OF CARDIOVASCULAR MAGNETIC RESONANCE®
Vol. 6, No. 2, pp. 527–539, 2004

ANGIOGRAPHY AND PERFUSION

Combined Coronary and Perfusion Cardiovascular Magnetic Resonance for the Assessment of Coronary Artery Stenosis

Nicholas H. Bunce,[1,*] Eliana Reyes,[1] Jennifer Keegan,[1] Catey Bunce,[3] Simon W. Davies,[2] Christine H. Lorenz,[1] and Dudley J. Pennell[1]

[1]Cardiovascular Magnetic Resonance Unit and [2]Department of Cardiology, Royal Brompton Hospital, London, UK
[3]Moorfields Eye Hospital, London, UK

ABSTRACT

The purpose of this study was to evaluate the feasibility and accuracy of combined coronary and perfusion cardiovascular magnetic resonance (CMR) in the assessment of coronary artery stenosis. Thirty-five consecutive patients (27 men, eight women, age range 34–81 years), undergoing cardiac catheterization, were assessed with 3D coronary CMR and rest-stress perfusion CMR. Significant coronary stenosis was determined by vessel narrowing or signal loss with coronary CMR, and by abnormal contrast enhancement with perfusion CMR. Coronary artery diameter stenosis greater than 50% was considered significant with conventional cardiac catheterization. Seventeen patients had significant coronary artery disease, and in these there were 35 significant stenoses on cardiac catheterization. All left main stem arteries were normal on both cardiac catheterization and coronary CMR. For the diagnosis of coronary artery stenosis, coronary CMR had a sensitivity of 92% for the left anterior descending artery (LAD), 79% for the right coronary artery (RCA), but only 13% for the circumflex coronary artery (LCX). Perfusion CMR had corresponding sensitivities of 69%, 86%, and 63%, respectively. For all arteries the accuracies for coronary and perfusion CMR were 67% and 72%, respectively. Combining coronary and perfusion CMR improved the accuracy to 77%. These data demonstrate that in patients with

*Correspondence: Dr. Nicholas H. Bunce, Royal Brompton Hospital, Sydney St., London, SW3 6NP, UK; Fax: 44-20-7351-8816; E-mail: nickbunce@hotmail.com.

DOI: 10.1081/JCMR-120030580

1097-6647 (Print); 1532-429X (Online)
www.dekker.com

suspected coronary artery disease, combined coronary and perfusion CMR is feasible, increases the accuracy of detection of significant coronary stenosis, and offers the possibility of combined anatomical and hemodynamic assessment of coronary artery stenosis.

Key Words: Cardiovascular magnetic resonance; Perfusion; Coronary artery stenosis.

INTRODUCTION

The development of coronary cardiovascular magnetic resonance (CMR) has enabled the noninvasive detection of significant epicardial coronary artery stenoses in patients with angina (Kim et al., 2001a). Initially, single-slice two-dimensional (2D) techniques were employed, but these required multiple breath-holds to image tortuous coronary arteries (Manning et al., 1993; Pennell et al., 1993; Post et al., 1997; Yoshino et al., 1997). The development of respiratory gating enabled the acquisition of three-dimensional (3D) volume slabs acquired over several minutes of free breathing (Huber et al., 1999; Kessler et al., 1999; Lethimonnier et al., 1999; Muller et al., 1997; Post et al., 1996; Sandstede et al., 1999; Van Geuns et al., 1999), or during a single breath-hold with the use of intravenous gadolinium-based contrast agents (Regenfus et al., 1999; Van Geuns et al., 1998). However, diagnostic accuracy and image quality may be reduced by residual respiratory artifacts and limited spatial resolution.

An alternative approach to the detection of a significant coronary stenosis is to measure myocardial perfusion or myocardial perfusion reserve with positron emission tomography (PET) (Demer et al., 1989; Uren et al., 1994) or single photon computed tomography (SPECT) (Go et al., 1990). More recently, the assessment of perfusion has been possible using CMR (Al-Saadi et al., 2000; Wilke et al., 1997). These studies have investigated the effects of an injection of gadolinium on the signal intensity of the myocardium before and after a coronary vasodilator. A significant coronary stenosis impairs the signal intensity increase after gadolinium, which can be detected either visually or semiquantitatively using signal-intensity time curves.

In this study, we evaluated the feasibility of performing both coronary and perfusion CMR in a population of patients with angina, for the combined anatomical and hemodynamic assessment of coronary stenosis. We also assessed if the combination of coronary and perfusion CMR improved the accuracy for the detection of proximal significant coronary artery stenosis.

MATERIALS AND METHODS

Patients

We recruited 35 consecutive patients (27 men, eight women, mean age 56 years, range 34–81) undergoing diagnostic cardiac catheterization for the investigation of angina (Table 1). The defined exclusion criteria were: an inability or unwillingness to give informed consent; unstable angina or recent myocardial infarction; the presence of an implanted permanent pacemaker, defibrillator, or intracranial clips; significant claustrophobia; bronchial asthma; or previous coronary artery bypass surgery. The study protocol was approved by the hospital Ethics Committee.

Cardiovascular Magnetic Resonance

Cardiovascular magnetic Resonance was performed using a Picker 1.5T Edge scanner (Cleveland, OH) with a four-channel phased array coil centered over the precordium with the patient in a supine position. For coronary CMR, initial 2D gradient-echo scans were obtained that included the origin of the right coronary artery from the right sinus of Valsalva and several arterial cross-sections during its course down the right atrio-ventricular sulcus. From these pilot scans an oblique coronal 3D slab was acquired that included an in-plane view of the right coronary artery. For the left coronary artery, 2D gradient-echo scans of the left sinus of Valsalva were acquired in both coronal and transverse planes, and from these an oblique transverse 3D slab was acquired that included the left main stem, left anterior descending, and circumflex arteries. A 3D segmented gradient-echo sequence was used with eight secondary phase encoding steps (kz) acquired per data segment. The limited gradient performance of the scanner resulted in this sequence having a relatively long echo time (TE) and repetition time (TR) (TE 4.3 ms, TR 12.9 ms). Although this has the disadvantage of extending the acquisition window (to 103 ms), the relatively long TE may be beneficial in determining the presence of stenoses by increasing the signal loss due to turbulent flow (Kilner et al., 1991). An

Table 1. Patient characteristics.

n	35
Sex, male/female	27/8
Age, y	56 ± 12
Risk factors, n (%)	
Systemic hypertension	12 (34)
Diabetes mellitus	3 (9)
Smoking	16 (46)
Positive family history	13 (37)
Symptoms, n (%)	
NYHA II	29 (83)
NYHA III	6 (17)
Coronary anatomy, n (%)	
Single vessel disease	4 (11)
Double vessel disease	8 (23)
Triple vessel disease	5 (14)
LMS stenosis	0 (0)
LAD stenosis	13 (37)
LCX stenosis	8 (23)
RCA stenosis	14 (40)
LVEF, %	61 ± 12

Note: Values are mean ± SD, or n (%). NYHA, New York Heart Association functional class; LVEF, left ventricular ejection fraction (angiography); stenosis >50% diameter reduction; LMS, left main stem; LAD, left anterior descending artery; LCX, circumflex coronary artery; RCA, right coronary artery.

incremental flip angle (20–90°) was used within the segment to improve signal-to-noise ratio. Eight secondary (k_z) and 128–192 primary phase encode acquisitions (k_y) were reformatted with a slab thickness of 20 mm and a field-of-view of 260–300 mm resulting in voxel dimensions of $1.0–1.2 \times 1.4–2.3 \times 2.5$ mm. A fat suppression pulse was used to suppress perivascular fat, and the acquisition window positioned in mid-to late-diastole to reduce cardiac motion artifact. For prospective respiratory gating, a navigator echo was generated from the intersection of orthogonal slice-selective 90° and 180° radio-frequency (RF) pulses positioned through the dome of the right hemi-diaphragm. The sequence was ordered using Hybrid Ordered Phase Encoding (Jhooti et al., 1998, 1999) to improve scan efficiency.

For perfusion CMR, initial pilot scans were acquired of the vertical and horizontal long axes of the heart, and used to position two short axis slices at one-third and two-thirds of the distance from the left ventricular apex to the base. An ultra-fast gradient-echo sequence was used (TE 1.2 ms, TR 3.0 ms), flip angle of 18°, phase matrix 64, slice thickness of 10 mm, field-of-view 500 by 250 mm yielding a pixel size of 3.9 by 3.9 mm, interpolated to 1.95 by 1.95 mm. With the patient performing shallow respiration, 0.05 mmol/kg gadolinium-DPTA (Magnevist, Schering AG, Berlin, Germany) and 15 mL 0.9% sodium chloride flush were injected at 10 mL/sec, through a peripheral cannula in the right antecubital fossa, using a power-injector (Spectris, Medrad, Inola, PA). The sequence was cardiac gated, acquiring both slices in a single R–R interval, with scan duration lasting 50 heartbeats. Resting perfusion CMR was performed after completion of the coronary CMR study. The patient was kept on the scanner table but removed from the magnet bore for 20 minutes to allow for clearance of the contrast agent from the myocardium. The patient was then repositioned in the identical position within the magnet bore, and adenosine was infused via a separate cannula at a rate of 140 µg/kg/min. After 6 minutes of pharmacological stress the perfusion CMR scan was repeated.

Cardiac catheterization was performed on all subjects within six months of CMR (range 1–157 days, median 27), with no significant cardiac event (myocardial infarction, unstable angina) occurring between the two imaging procedures. Cardiac catheterization was performed using the standard Judkins technique (Judkins, 1967) with selective catheterization of the right and left coronary arteries. Coronary stenosis was defined visually as a ≥50% luminal diameter reduction, for each segment of the arterial tree, using the American Heart Association classification (Scanlon et al., 1999).

Analysis and Statistics

All the CMR images were transferred to a computer workstation and analyzed using CMRtools (©Imperial College, London). Both coronary and perfusion CMR were analysed by two experienced observers blinded to patient identity and the results from the previous imaging modality. Cardiac catheterization was the reference standard for the diagnosis of a significant coronary artery stenosis, and a correct diagnosis was assigned to CMR if the significant stenosis corresponded to the same arterial segment or territory. A visual scoring scale was used as follows: 0, very poor (images insufficient for analysis of coronary stenosis or perfusion abnormality because of blurring or major artifacts); 1, poor (coronary arteries or myocardium could barely be detected on the images); 2, adequate (images sufficient for analysis but with major blurring or artifacts); 3, good (images sufficient for analysis but with minor blurring or artifacts); 4, excellent (no blurring and no artifacts).

For coronary CMR, arterial anatomy was defined according to the American Heart Association Guidelines

(Scanlon et al., 1999). The right coronary artery (RCA) corresponded to cardiac catheterization segments 1, 2, and 3; the left main stem artery (LMS), segment 11; the left anterior descending artery (LAD), segments 12 and 13; and the circumflex coronary artery (LCX), segment 18. Each artery was assessed for the presence of a significant stenosis as defined by vessel narrowing or signal loss within an arterial segment. For coronary CMR, each artery was classified as normal or stenosed.

For perfusion CMR an initial visual assessment was performed by displaying the rest and stress cines for both slices. Each myocardial short axis slice was divided into eight equal segments using the junction between the interventricular septum and the right ventricle as a fixed point. Segments were assigned to the anatomical distribution of the left anterior descending, circumflex artery, and right coronary arteries, with arterial dominance determined by cardiac catheterization. The endocardial region was traced, being careful to avoid the blood pool, and the mean signal intensity measured within each region was determined. To correct for the proximity of each region from the receiver coils, the values obtained during administration of gadolinium were divided by the baseline value precontrast. Signal intensity curves over time were then obtained for each region of interest and the upslope determined. In each patient the upslope obtained was normalized to the maximum within a single short-axis slice. A reference range (median and percentiles) was obtained for each region of interest in the patients with normal coronary arteries. This range was then applied to the study population when determining the diagnostic accuracy for the detection of coronary artery stenosis.

Image quality for coronary and perfusion CMR were compared using the Wilcoxon Signed Rank Test. For both coronary and perfusion CMR, images with a visual score of 2 or above (adequate) were considered correct, but images rated 1 or below were considered uninterpretable and labeled incorrect for subsequent analysis. As there were no significant left main stem artery stenoses identified by cardiac catheterization or coronary CMR, these arteries were not included in the formal analysis. For coronary and perfusion CMR, the sensitivity, specificity, accuracy, and 95% confidence intervals (CI) were obtained for each vessel. In addition, a combined assessment was then performed.

RESULTS

On cardiac catheterization, 17 patients had significant coronary artery stenoses, and there were 35 significant stenoses (Table 1). Three-vessel coronary artery disease was detected in five patients, another eight patients had two-vessel disease, and four patients had single vessel coronary artery disease. All 35 patients completed the CMR protocol, with a mean total acquisition time of 62 minutes (range 49–92). Coronary CMR acquisition duration was determined by the stability of the respiratory breathing pattern during the scan and the resting heart rate. Patients with the most stable respiratory pattern and a relatively fast heart rate completed the scans in the shortest amount of time. Perfusion CMR acquisition duration was determined by the heart rate (50 heartbeats).

All the left main stem arteries were normal on cardiac catheterization and correctly identified with coronary CMR and were not included for formal analysis. Of 13 significant stenoses in the left anterior descending artery, 12 were correctly identified by coronary CMR (sensitivity 92%, specificity 73%), compared to nine by perfusion CMR (sensitivity 69%, specificity 59%) (Table 2). For the circumflex coronary artery, coronary CMR performed less well identifying only one out of eight significant stenoses (sensitivity 13%, specificity 56%), but perfusion CMR identified five out of eight significant stenoses (sensitivity 63%,

Table 2. The detection of the coronary artery stenoses by coronary CMR, perfusion CMR, and the combined assessment with coronary-perfusion CMR.

	Coronary CMR			Perfusion CMR			Combined		
	Sens	Spec	Acc	Sens	Spec	Acc	Sens	Spec	Acc
LAD	92 (64,100)	73 (50,89)	80 (63,92)	69 (39,91)	59 (36,79)	63 (45,79)	62 (32,86)	91 (71,99)	80 (63,92)
LCX	13 (0,53)	56 (39,78)	49 (31,66)	63 (24,91)	70 (50,86)	69 (51,83)	63# (24,91)	70# (50,86)	69# (51,83)
RCA	79 (49,95)	67 (43,85)	71 (54,85)	86 (57,98)	86 (64,97)	85 (70,95)	64 (35,87)	95 (76,100)	83 (66,93)
ALL	68 (51,83)	66 (53,77)	67 (57,76)	74 (57,88)	71 (59,82)	72 (63,81)	63 (45,79)	84 (74,92)	77 (68,85)

Note: The figures are percentages and with the 95% confidence intervals in parenthesis (#—the values obtained for the combined assessment for LCX represent the contribution of perfusion CMR only—see text for explanation.)

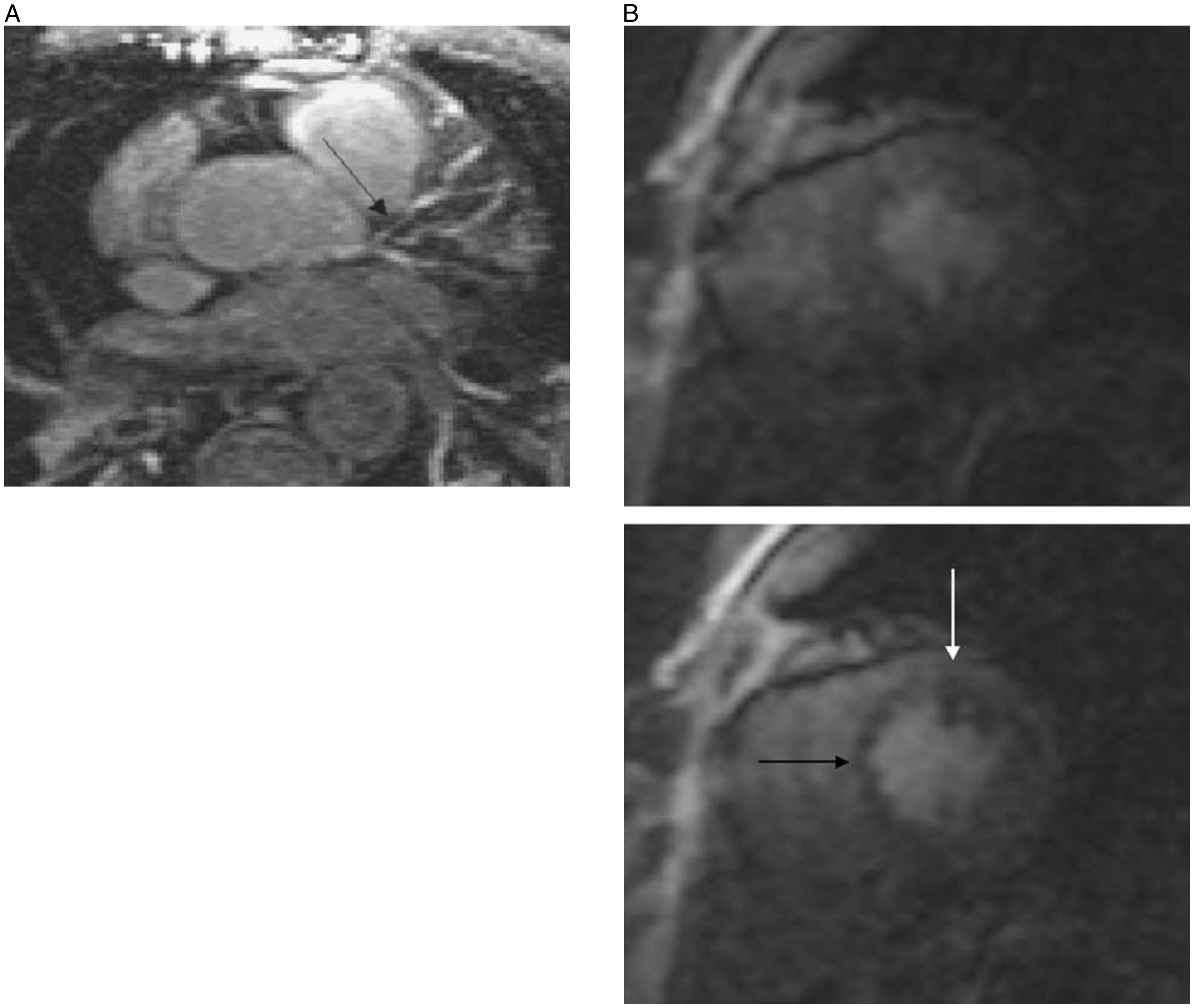

Figure 1. A 3D-rendered coronary CMR (A) of vessel narrowing in the proximal left anterior descending artery that was classified as a significant coronary stenosis. At baseline there is homogenous perfusion CMR (B, top panel), in the left ventricular short-axis slice. With adenosine stress (B, lower panel), there are perfusion defects in the antero-septum and anterior wall consistent with a significant stenosis of the left anterior descending artery. Signal intensity over time curves (C) demonstrate that following chemical stress there is marked increase in the upslope for the inferior wall (upper panel) compared to the septum (lower panel). Cardiac catheterization (D, left anterior oblique, LAO, view with cranial angulation) confirmed a significant proximal left anterior descending artery stenosis.

(continued)

specificity 70%). For the right coronary artery coronary, CMR detected 11 out of 14 significant stenoses (sensitivity 79%, specificity 67%), compared to 12 by perfusion CMR (sensitivity 86%, specificity 86%).

The combination of coronary and perfusion CMR was performed using the following protocol:

- Perfusion CMR analysis was first applied to identify arterial territories with abnormal stress perfusion.
- Coronary CMR analysis was secondly applied to regions with abnormal stress perfusion to confirm or to refute the presence of a coronary stenosis.
- Because the coronary CMR results were unsatisfactory for the circumflex coronary artery, the perfusion CMR was used alone for this territory.

Applying the protocol for all vessels, the diagnostic accuracy (relative to cardiac catheterization) could be

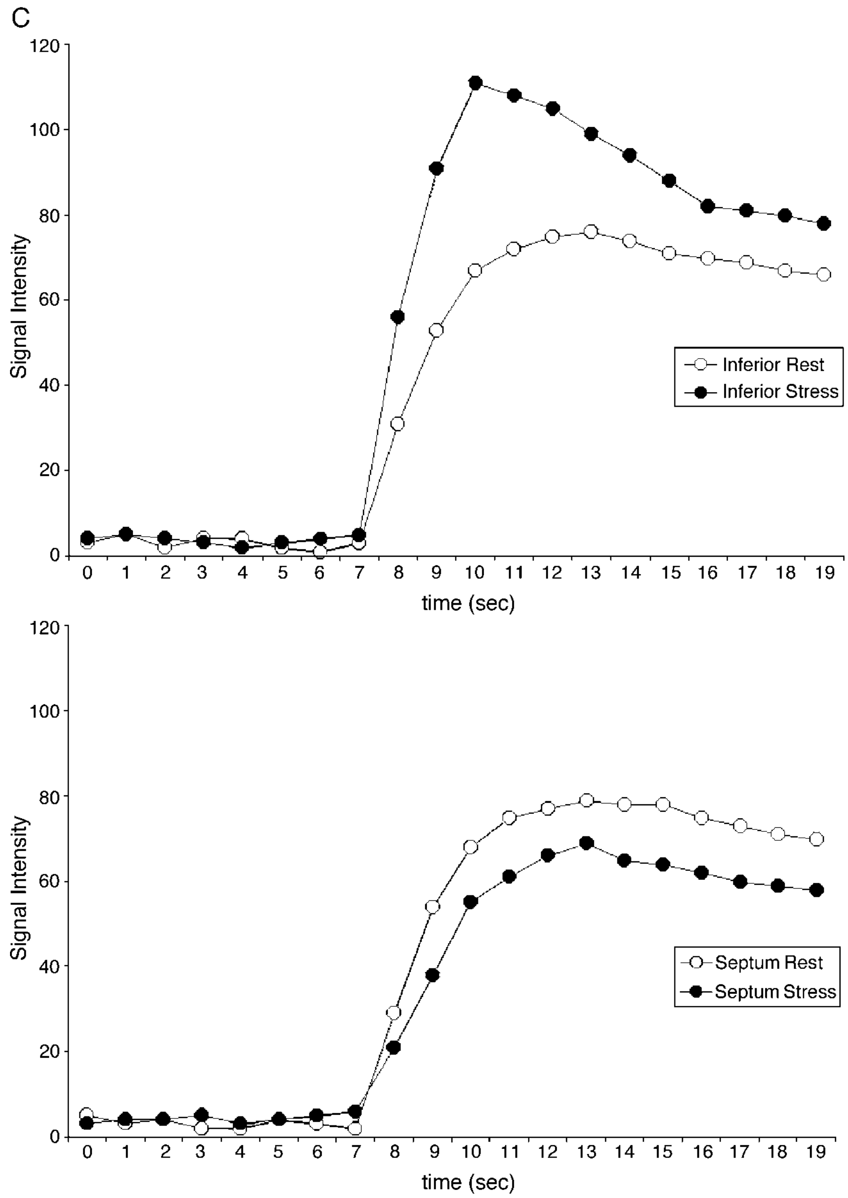

Figure 1. Continued.

improved from 67% (coronary CMR alone) and 72% (perfusion CMR alone) to 77% (combined, Table 2).

The mean visual scores were similar for both coronary CMR and perfusion CMR, apart from the circumflex coronary artery, which was significantly worse when imaged by coronary CMR ($p < 0.05$). Improved image quality was associated with a correct diagnosis with both coronary CMR and perfusion CMR, although this only reached statistical significance for perfusion CMR ($p < 0.05$). Figures 1 and 2 demonstrate the complementary assessment of coronary artery stenosis by coronary CMR and perfusion CMR.

DISCUSSION

The accurate detection of coronary artery stenosis by coronary CMR has been the stimulus behind many developments in the field of cardiovascular magnetic resonance. Early investigators used single-slice segmented gradient-echo techniques to identify coronary arteries and stenoses (Manning et al., 1993; Pennell et al., 1993; Post et al., 1997). These 2D acquisitions, obtained during breath-holding, required multiple breath-holds for a complete study of an artery and so were subject to the problems of limited resolution, slice

D

Figure 1. Continued.

misregistration, and required considerable patient cooperation (Taylor et al., 1999). However, it was still possible to obtain high sensitivities for the detection of coronary artery stenoses (63–100%) (Manning et al., 1993; Pennell et al., 1993; Post et al., 1997; Yoshino et al., 1997). With the development of respiratory navigators, which enabled free-breathing acquisitions, it became possible to obtain a complete 3D data set of a coronary artery within several minutes. When used for studies of coronary artery disease patients, slightly lower sensitivities (38–83%) were obtained than for the 2D methods, due to residual respiratory and motion artifacts (Huber et al., 1999; Kessler et al., 1999; Lethimonnier et al., 1999; Muller et al., 1997; Post et al., 1996; Sandstede et al., 1999; Van Geuns et al., 1999). We have previously used free-breathing prospective navigator-gated coronary CMR in patients with suspected coronary artery disease with good accuracy for the left anterior descending and right coronary arteries (Bunce et al., 2001). A recent multicenter trial using a 3D sequence with respiratory navigators showed good results for the exclusion of significant coronary disease, but overall accuracy was still only 72% (Kim et al., 2001a).

By contrast, the assessment of myocardial perfusion forms the basis of noninvasive methods of diagnosing coronary artery disease such as SPECT (Elhendy et al., 2000a,b; Go et al., 1990; Kim et al., 2001b), PET (Demer et al., 1989; Uren et al., 1994), and more recently by echocardiography (Elhendy et al., 1998; Santoro et al., 1998) and CMR (Al-Saadi et al., 2001; Cullen et al., 1999; Ibrahim et al., 2002; Keijer et al., 2000; Panting et al., 2002; Sensky et al., 2002). These methods use a stressor agent, e.g., adenosine, dipyridamole, or dobutamine, to produce coronary vasodilation. Myocardium supplied by a stenosed coronary artery may have normal perfusion at rest, but when subjected to vasodilation, the expected increase in perfusion is reduced according to the severity of the coronary artery stenosis. Cardiovascular magnetic resonance is able to study this effect, using the myocardial signal intensity increase that results from the first-pass effects of an injection of gadolinium. The increase in myocardial signal intensity is reduced or delayed in the presence of a significant stenosis, and this can be demonstrated either visually or with a quantitative analysis of the signal upslope. This method has been used in small studies of patients with coronary artery disease, with good reported sensitivities (Al-Saadi et al., 2000; Schwitter et al., 2001). The perfusion CMR sequence used in this study has recently been used to identify subendocardial perfusion abnormalities in patients with cardiac syndrome X (Panting et al., 1948).

Dobutamine CMR and the assessment of stress-induced regional wall motion abnormalities can also be used to diagnose coronary artery stenoses (Pennell et al., 1992). In recent studies, dobutamine CMR accurately predicted the presence of significant coronary artery stenoses (Kuijpers et al., 2003; Nagel et al., 1999). However, the magnetic field does limit interpretation of the 12-lead electrocardiogram, and high-dose dobutamine can cause ventricular arrhythymias including ventricular fibrillation (Kuijpers et al., 2003). The dose-titration of dobutamine may also prolong the study acquisition as compared to adenosine (Kuijpers et al., 2003).

In this study we investigated the feasibility of a protocol that consisted of a combined coronary and perfusion CMR for combined anatomical and hemodynamic assessment of coronary stenoses. This proved feasible in all patients and was well tolerated taking approximately 60 minutes. When assessed alone, coronary CMR was sensitive for the detection of significant coronary stenoses in both the left anterior descending and right coronary arteries (92% and 79%, respectively), with specificities for of 73% and 67%, respectively. However, coronary CMR performed less well in the assessment of the circumflex coronary artery with a sensitivity of only 13%. This may be explained by the fact that the circumflex coronary artery is the most posteriorly located artery, and signal-to-noise deteriorates as the distance from the surface coil increases. The acquisition of a separate oblique slab

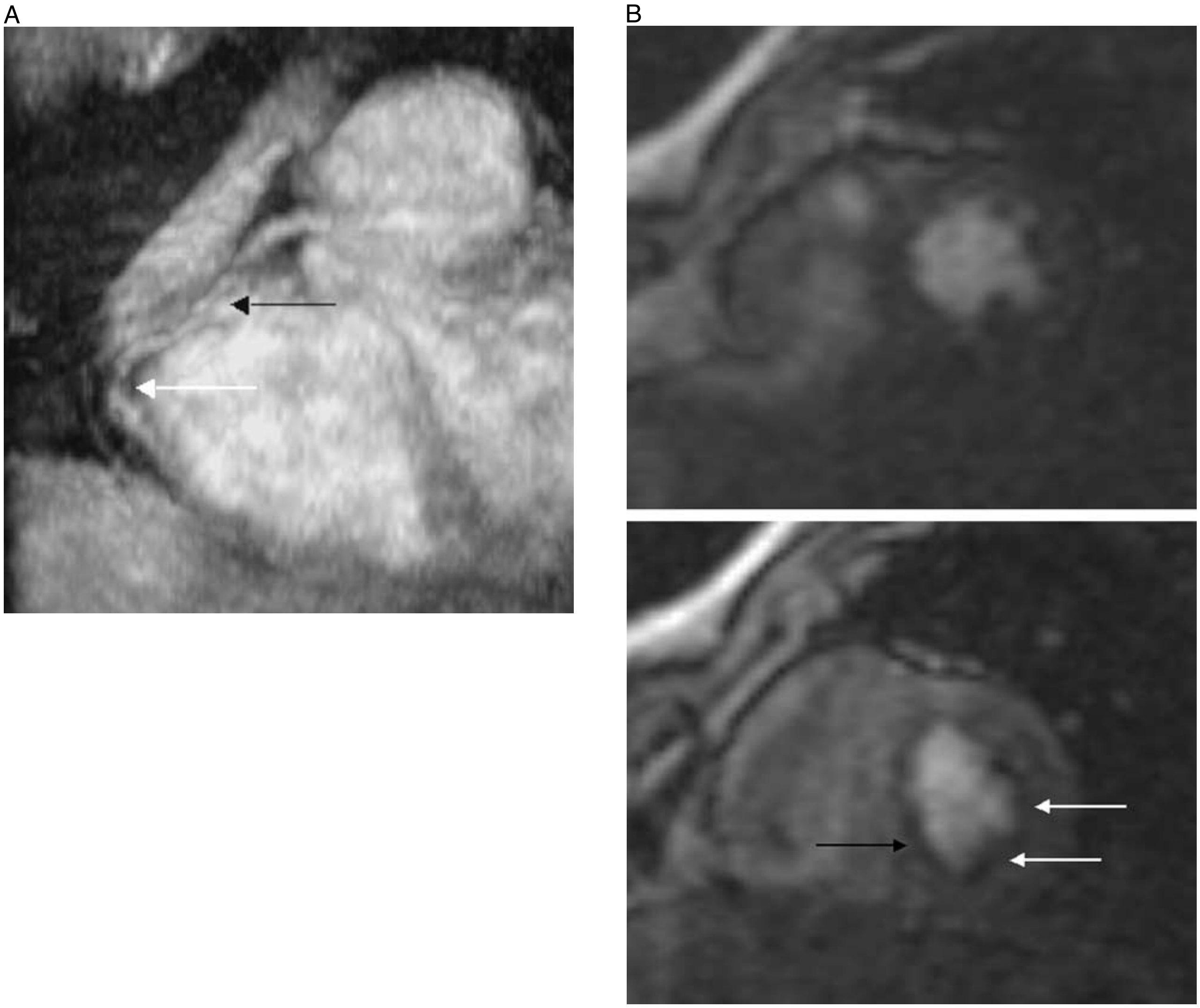

Figure 2. A 3D-rendered coronary CMR (A) of an area of vessel narrowing of the proximal right coronary artery (black arrow) and more distally signal loss (white arrow) that was classified as a significant coronary stenosis. At baseline there is homogenous perfusion CMR (B, top panel) in the left ventricular short axis slice. With adenosine stress (B, lower panel), there are perfusion defects in the infero-septum and inferior wall (black arrow) and the lateral wall (white arrows) consistent with significant stenoses of the right and circumflex coronary arteries. Signal intensity over time curves (C) demonstrate that following chemical stress there is marked increase in the upslope for the anterior wall (upper panel) compared to the inferior and lateral walls (lower panel). Cardiac catheterization (D, LAO straight view) confirmed a significant stenosis in the right coronary artery (white arrow) that corresponds to the stenosis identified with coronary and perfusion CMR, and an additional significant stenosis in the circumflex coronary artery (D, right anterior oblique, RAO, straight view, black arrow) demonstrated only by perfusion CMR.

for the circumflex coronary artery may improve the sensitivity for coronary CMR (Van Geuns et al., 2000; Watanabe et al., 2002). However, even with a volume-targeted approach, nearly half of proximal circumflex coronary arteries will be nonassessable (Van Geuns et al., 2000).

In this study, using perfusion CMR alone produced sensitivities of 62% for the left anterior descending artery, 63% for the circumflex coronary artery, and 86% for the right coronary artery. Specificity was 59%, 70%, and 86% respectively. When the results of the coronary CMR and perfusion CMR were combined, the diagnostic accuracy improved from 67% (coronary CMR) and 72% (perfusion CMR) to a maximum of 77% (combined coronary CMR and perfusion CMR, Table 2).

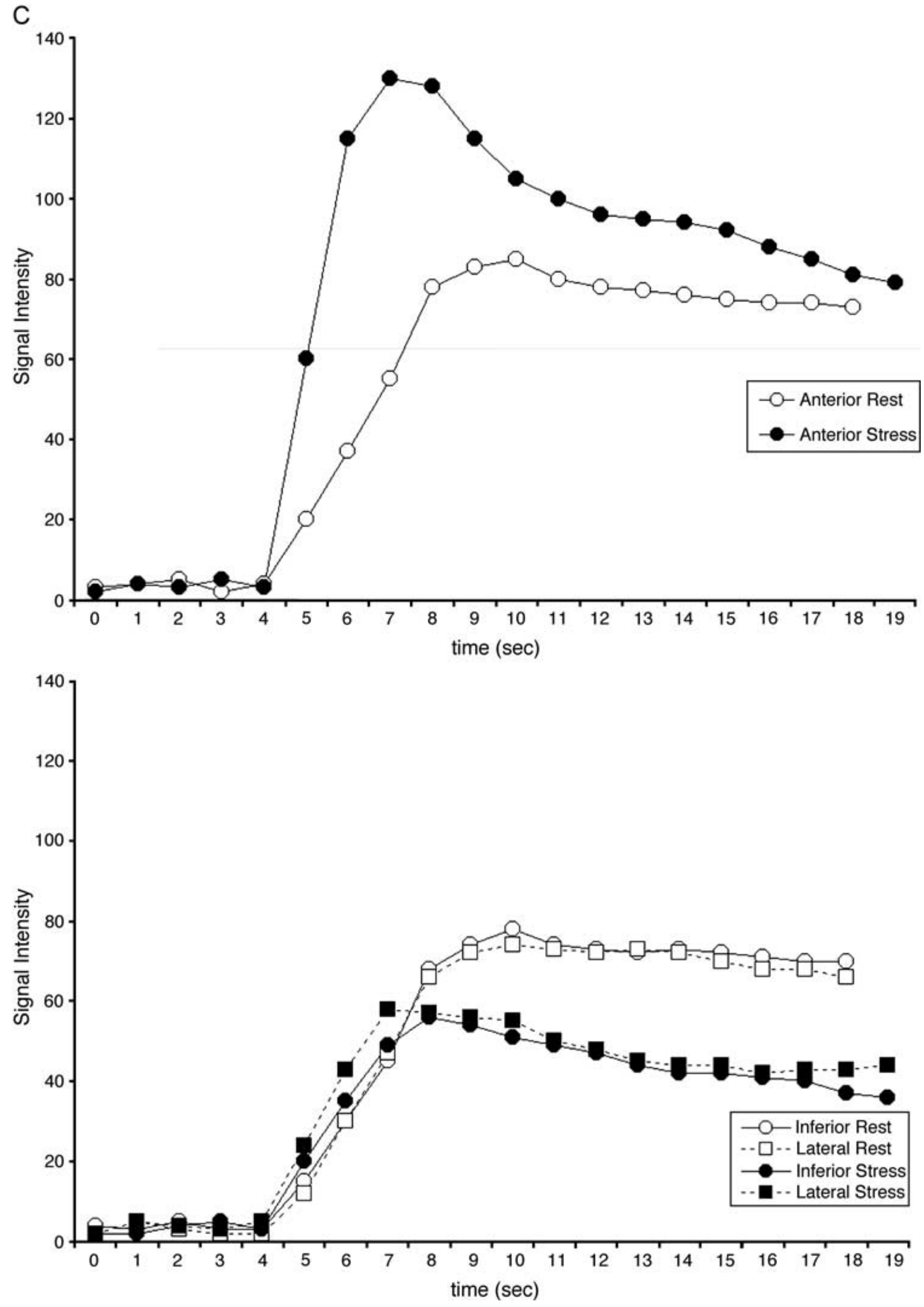

Figure 2. Continued.

(continued)

Limitations

- In this study the patients were removed from the magnet bore between the rest and the stress images. The patients were returned to isocenter but there is potential for slice misregistration that may reduce the accuracy of perfusion CMR analysis. During the delay between the rest and stress images it would be possible to obtain functional (wall-motion) (Poon et al., 2002;

D

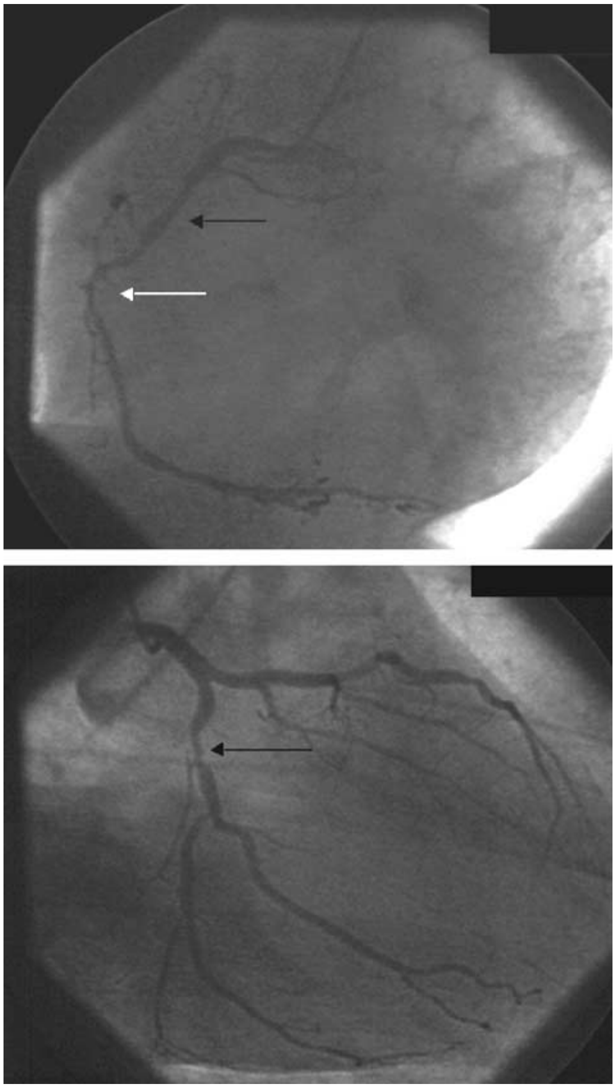

Figure 2. Continued.

Sensky et al., 2000) and viability (delayed-enhancement) (Beek et al., 2003; Kim et al., 2000) data that may provide additional diagnostic information.

- The definition of a significant coronary artery stenosis on cardiac catheterization was performed by visual assessment only and may have been improved by quantitative coronary angiography. Although cardiac catheterization was considered the standard of reference for the assessment of coronary artery stenoses, myocardial perfusion abnormalities may be better assessed with PET or SPECT techniques, which could have been used to determine the accuracy of perfusion CMR.

CONCLUSION

The combined protocol of coronary CMR and perfusion CMR was well tolerated by our patient group with no adverse effects, and was feasible in less than 90 minutes. The combination of coronary and perfusion CMR improved the diagnostic accuracy for the detection of coronary artery stenoses in patients with angina. Improvements in respiratory suppression may further increase the accuracy of coronary CMR, while technical advances and increasing the coverage of myocardium assessed by perfusion CMR may improve its sensitivity. This protocol is straightforward, and the results from this study should be formally assessed in a larger prospective trial.

REFERENCES

Al-Saadi, N., Nagel, E., Gross, M., Bornstedt, A., Schnackenburg, B., Klein, C., Klimek, W., Oswald, H., Fleck, E. (2000). Noninvasive detection of myocardial ischemia from perfusion reserve based on cardiovascular magnetic resonance. *Circulation* 101:1379–1383.

Al-Saadi, N., Gross, M., Bornstedt, A., Schnackenburg, B., Klein, C., Fleck, E., Nagel, E. (2001). Comparison of various parameters for determining an index of myocardial perfusion reserve in detecting coronary stenosis with cardiovascular magnetic resonance tomography. *Z. Kardiol.* 90 (11):824–834.

Beek, A. M., Kuhl, H. P., Bondarenko, O., Twisk, J. W., Hofman, M. B., van Dockum, W. G., Visser, C. A., van Rossum, A. C. (2003). Delayed contrast-enhanced magnetic resonance imaging for the prediction of regional functional improvement after acute myocardial infarction. *J. Am. Coll. Cardiol.* 42:895–901.

Bunce, N. H., Jhooti, P., Keegan, J., Rahman, S. L., Bunce, C., Firmin, D. N., Davies, S. W., Lorenz, C. H., Pennell, D. J. (2001). Evaluation of free-breathing three-dimensional magnetic resonance coronary angiography with hybrid ordered phase encoding (HOPE) for the detection of proximal coronary artery stenosis. *J. Magn. Reson. Imaging* 14:677–684.

Cullen, J. H., Horsfield, M. A., Reek, C. R., Cherryman, G. R., Barnett, D. B., Samani, N. J. (1999). A myocardial perfusion reserve index in humans using first-pass contrast-enhanced magnetic resonance imaging. *J. Am. Coll. Cardiol.* 33:1386–1394.

Demer, L. L., Gould, K. L., Goldstein, R. A., Kirkeeide, R. L., Mullani, N. A., Smalling, R. W., Nishikawa, A., Merhige, M. E. (1989). Assessment of coronary artery disease severity by positron emission tomography: comparison with quantitative coronary angiography in 193 patients. *Circulation* 79:825–835.

Elhendy, A., van Domburg, R. T., Bax, J. J., Poldermans, D., Nierop, P. R., Kasprzak, J. D., Roelandt, J. R. (1998). Optimal criteria for the diagnosis of coronary artery disease by dobutamine stress echocardiography. *Am. J. Cardiol.* 82:1339–1344.

Elhendy, A., Sozzi, F. B., van Domburg, R. T., Bax, J. J., Geleijnse, M. L., Valkema, R., Krenning, E. P., Roelandt, J. R. (2000a). Accuracy of exercise stress technetium 99m sestamibi SPECT imaging in the evaluation of the extent and location of coronary artery disease in patients with an earlier myocardial infarction. *J. Nucl. Cardiol.* 7:432–438.

Elhendy, A., Sozzi, F. B., Valkema, R., van Domburg, R. T., Bax, J. J., Roelandt, J. R. (2000b). Dobutamine technetium-99m tetrofosmin SPECT imaging for the diagnosis of coronary artery disease in patients with limited exercise capacity. *J. Nucl. Cardiol.* 7:649–654.

Go, R. T., Marwick, T. H., MacIntyre, W. J., Saha, G. B., Neumann, D. R., Underwood, D. A., Simpfendorfer, C. C. (1990). A prospective comparison of rubidium 82 PET and thallium 201 SPECT myocardial perfusion imaging utilising a single dipyridamole stress in the diagnosis of coronary artery disease. *J. Nucl. Med.* 31:1899–1905.

Huber, A., Nikolau, K., Gonschior, P., Knez, A., Stehling, M., Reiser, M. (1999). Navigator echo-based respiratory gating for three-dimensional MR coronary angiography: results from healthy volunteers and patients with proximal coronary artery stenoses. *Am. J. Roentgenol.* 173:95–101.

Ibrahim, T., Nekolla, S. G., Schreiber, K., Odaka, K., Volz, S., Mehilli, J., Guthlin, M., Delius, W., Schwaiger, M. (2002). Assessment of coronary flow reserve: comparison between contrast-enhanced magnetic resonance imaging and positron emission tomography. *J. Am. Coll. Cardiol.* 39:864–870.

Jhooti, P., Wiesmann, F., Taylor, A. M., Gatehouse, P. D., Yang, G. Z., Keegan, J., Pennell, D. J., Firmin, D. N. (1998). Hybrid ordered phase encoding (HOPE): an improved approach for respiratory artifact reduction. *J. Magn. Reson. Imaging* 8:968–980.

Jhooti, P., Keegan, J., Gatehouse, P. D., Collins, S., Rowe, A., Taylor, A. M., Firmin, D. N. (1999). 3D coronary artery imaging with phase reordering for improved scan efficiency. *Magn. Reson. Med.* 41:555–562.

Judkins, M. P. (1967). Selective coronary arteriography. I: a percutaneous transfemoral technique. *Radiology* 89:815–824.

Keijer, J. T., van Rossum, A. C., Wilke, N., van Eenige, M. J., Jerosch-Herold, M., Bronzwaer, J. G., Visser, C. A. (2000). Magnetic resonance imaging of myocardial perfusion in single-vessel coronary artery disease: implications for transmural assessment of myocardial perfusion. *J. Cardiovasc. Magn. Reson.* 2:189–200.

Kessler, W., Laub, G., Achenbach, S., Ropers, D., Moshage, W., Daniel, W. G. (1999). Coronary arteries: MR angiography with fast contrast-enhanced three-dimensional breath-hold imaging-initial experience. *Radiology* 210:566–572.

Kilner, P. J., Firmin, D. N., Rees, R. S., Martinez, J., Pennell, D. J., Mohiaddin, R. H., Underwood, S. R., Longmore, D. B. (1991). Valve and great vessel stenosis: assessment with MR jet velocity mapping. *Radiology* 178:229–235.

Kim, R. J., Wu, E., Rafael, A., Chen, E. L., Parker, M. A., Simonetti, O., Klocke, F. J., Bonow, R. O., Judd, R. M. (2000). The use of contrast-enhanced magnetic resonance imaging to identify reversible myocardial dysfunction. *N. Engl. J. Med.* 343:1445–1453.

Kim, W. Y., Danias, P. G., Stuber, M., Flamm, S. D., Plein, S., Nagel, E., Langerak, S. E., Weber, O. M., Pedersen, E. M., Schmidt, M., Botnar, R. M., Manning, W. J. (2001a). Coronary magnetic resonance angiography for the detection of coronary stenoses. *N. Engl. J. Med.* 345:1863–1869.

Kim, C., Kwok, Y. S., Heagerty, P., Redberg, R. (2001b). Pharmacologic stress testing for coronary disease diagnosis: a meta-analysis. *Am. Heart J.* 142:934–944.

Kuijpers, D., Yiu, K., Ho, J. A. M., van Dijkman, P. R. M., Vliegenthart, R., Oudkerk, M. (2003). Dobutamine cardiovascular magnetic resonance for the detection of myocardial ischemia with the use of myocardial tagging. *Circulation* 107:1592–1597.

Lethimonnier, F., Furber, A., Morel, O., Geslin, P., L'Hoste, P., Tadei, A., Jallet, P., Caron-Poitreau, C., Le Jeune, J. J. (1999). Three-dimensional coronary artery MR imaging using prospective real-time respiratory navigator and linear phase shift processing: comparison with conventional coronary angiography. *Magn. Reson. Imaging* 17:1111–1120.

Manning, W. J., Li, W., Edelman, R. R. (1993). A preliminary report comparing magnetic resonance coronary angiography with conventional angiography. *N. Engl. J. Med.* 328:828–832.

Muller, M. F., Fleisch, M., Kroeker, R., Chatterjee, T., Meier, B., Vock, P. (1997). Proximal coronary artery stenosis: three-dimensional MRI with fat saturation and navigator echo. *J. Magn. Reson. Imaging.* 7:644–651.

Nagel, E., Lehmkuhl, H. B., Bocksch, W., Klein, C., Vogel, U., Frantz, E., Ellmer, A., Dreysse, S., Fleck, E. (1999). Noninvasive diagnosis of ischemia-induced wall motion abnormalities with the use of high-dose dobutamine stress MRI comparison with dobutamine stress echocardiography. *Circulation* 99:763–770.

Panting, J. R., Gatehouse, P. D., Yang, G. Z., Grothues, F., Firmin, D. N., Collins, P., Pennell, D. J. (2002). Abnormal subendocardial perfusion in cardiac syndrome X detected by cardiovascular magnetic resonance imaging. *N. Engl. J. Med.* 346:1948–1953.

Pennell, D. J., Underwood, S. R., Manzara, C. C., Swanton, R. H., Walker, J. M., Ell, P. J., Longmore, D. B. (1992). Magnetic resonance imaging during dobutamine stress in coronary artery disease. *Am. J. Cardiol.* 70:34–40.

Pennell, D. J., Keegan, J., Firmin, D. N., Gatehouse, P. D., Underwood, S. R., Longmore, D. B. (1993). Magnetic resonance imaging of coronaries: technique and preliminary results. *Br. Heart. J.* 70:315–326.

Poon, M., Fuster, V., Fayad, Z. (2002). Cardiac magnetic resonance imaging: a ‘‘one-stop-shop’’ evaluation of myocardial dysfunction. *Curr. Opin. Cardiol.* 17:663–670.

Post, J. C., van Rossum, A. C., Hofman, M. B. M., Valk, J., Visser, C. A. (1996). Three-dimensional respiratory-gated MR angiography of coronary arteries: comparison with conventional contrast coronary angiography. *Am. J. Roentgenol.* 166: 426–433.

Post, J. C., van Rossum, A. C., Hofman, M. B. M., de Cock, C. C., Valk, J., Visser, C. A. (1997). Clinical utility of two-dimensional magnetic resonance angiography in detecting coronary artery disease. *Eur. Heart. J.* 18:426–433.

Regenfus, M., Ropers, D., Achenbach, S., Kessler, W., Moshage, W., Daniel, W. G. (1999). Gadolinium-enhanced 3D breath-hold magnetic resonance angiography for detection of coronary artery stenosis in oblique projection angiograms. Abstracts of the 7th Meeting of the International Society of Magnetic Resonance in Medicine. In: Proceedings of the 7th Scientific Meeting and Exhibition of the ISMRM. Philadelphia, PA, W1262.

Sandstede, J. J. W., Pabst, T., Beer, M., Geis, N., Kenn, W., Neubauer, S., Hahn, D. (1999). Three-dimensional MR coronary angiography using the navigator technique compared with conventional coronary angiography. *Am. J. Roentgenol.* 172:135–139.

Santoro, G. M., Sciagra, R., Buonamici, P., Consoli, N., Mazzoni, V., Zerauschek, F., Bisi, G., Fazzini, P. F. (1998). Head-to-head comparison of exercise stress testing, pharmacologic stress echocardiography, and perfusion tomography as first-line examination for chest pain in patients without history of coronary artery disease. *J. Nucl. Cardiol.* 5:19–27.

Scanlon, P. J., Faxon, D. P., Audet, A. M., Carabello, B., Dehmer, G. J., Eagle, K. A., Legako, R. D., Leon, D. F., Murray, J. A., Nissen, S. D., Pepine, C. J., Watson, R. M. (1999). ACC/AHA guidelines for coronary angiography: a report of the American college of cardiology/american heart association task force on practice guidelines (Committee on Coronary Angiography). *J. Am. Coll. Cardiol.* 33:1756–1782.

Schwitter, J., Nanz, D., Kneifel, S., Bertschinger, K., Buchi, M., Knusel, P. R., Marincek, B., Luscher, T. F., von Schulthess, G. K. (2001). Assessment of myocardial perfusion in coronary artery disease by magnetic resonance: a comparison with positron emission tomography and coronary angiography. *Circulation* 103:2230–2235.

Sensky, P. R., Jivan, A., Hudson, N. M., Keal, R. P., Morgan, B., Tranter, J. L., de Bono, D., Samani, N. J., Cherryman, G. R. (2000). Coronary artery disease: combined stress MR imaging protocol-one-stop evaluation of myocardial perfusion and function. *Radiology* 215:608–614.

Sensky, P. R., Samani, N. J., Horsfield, M. A., Cherryman, G. R. (2002). Restoration of myocardial blood flow following percutaneous coronary balloon dilatation and stent implantation: assessment with qualitative and quantitative contrast-enhanced magnetic resonance imaging. *Clin. Radiol.* 57:593–599.

Taylor, A. M., Keegan, J., Jhooti, P., Gatehouse, P. D., Firmin, D. N., Pennell, D. J. (1999). Differences between normal subjects and patients with coronary artery disease for three different MR coronary angiography respiratory suppression techniques. *J. Magn. Reson. Imaging* 9:786–793.

Uren, N. G., Melin, J. A., De Bruyne, B., Wijns, W., Baudhuin, T., Camici, P. G. (1994). Relation between myocardial blood flow and the severity of coronary-artery stenosis. *N. Engl. J. Med.* 330:1782–1788.

Van Geuns, R. J. M., Wieloposki, P. A., de Bruin, H. G., van Ooijen, P. M. A., Oudkerk, M., de Feyter, P. J. (1998). VCATS: volume coronary angiography using targeted scans, a new strategy in MR coronary angiography. *Circulation* 98:I-856.

Van Geuns, R. J. M., de Bruin, H. G., Rensing, B. J. W. M., Wielopolski, P. A., Hulshoff, M. D., van Ooijen, P. M. A., Oudkerk, M., de Feyter, P. J. (1999). Magnetic resonance imaging of the coronary arteries: clinical evaluation of a respiratory gated technique. *Heart* 82:515–519.

Van Geuns, R. J., Wielopolski, P. A., de Bruin, H. G., Rensing, B. J., Hulshoff, M., van Ooijen, P. M., de Feyter, P. J., Oudkerk, M. (2000). MR coronary angiography with breath-hold targeted volumes: preliminary clinical results. *Radiology* 217:270–277.

Watanabe, Y., Nagayama, M., Amoh, Y., Fujii, M., Fuku, Y., Okumura, A., Van Cauteren, M., Stuber, M., Dodo, Y. (2002). High-resolution selective three-dimensional magnetic resonance coronary angiography with navigator-echo technique: segment-by-segment evaluation of coronary artery stenosis. *J. Magn. Reson. Imaging* 16:238–245.

Wilke, N., Jerosch Herold, M., Wang, Y., Huang, Y., Christensen, B. V., Stillman, A. E., Ugurbil, K., McDonald, K., Wilson, R. F. (1997). Myocardial perfusion reserve: assessment with multisection, quantitative, first-pass MR imaging. *Radiology* 204:373–384.

Yoshino, H., Nitatori, T., Kachi, E., Yano, K., Taniuchi, M., Hachiya, J., Ishikawa, K. (1997). Directed proximal magnetic resonance angiography compared with conventional contrast coronary angiography. *Am. J. Cardiol.* 80:514–518.

Received July 9, 2003
Accepted November 23, 2003